Nuclear Instruments and Methods in Physics Research A 745 (2014) 114–118

Contents lists available at ScienceDirect

Nuclear Instruments and Methods in Physics Research A

journal homepage: www.elsevier.com/locate/nima

Extended calibration range for prompt photon emission in ion beam irradiation

F. Bellini [a,b], T.T. Boehlen [c], M.P.W. Chin [c], F. Collamati [a,b], E. De Lucia [d], R. Faccini [a,b,*], A. Ferrari [c], L. Lanza [a,b], C. Mancini-Terracciano [c,f], M. Marafini [e,b], I. Mattei [f,d], S. Morganti [b], P.G. Ortega [c], V. Patera [g,b], L. Piersanti [g,d], A. Russomando [h,b], P.R. Sala [i], A. Sarti [g,d], A. Sciubba [g,b], E. Solfaroli Camillocci [h], C. Voena [b]

[a] Dipartimento di Fisica, Sapienza Università di Roma, Roma, Italy
[b] INFN Sezione di Roma, Roma, Italy
[c] CERN, Geneva, Switzerland
[d] Laboratori Nazionali di Frascati dell'INFN, Frascati, Italy
[f] Dipartimento di Fisica, Università Roma Tre, Roma, Italy
[e] Museo Storico della Fisica e Centro Studi e Ricerche "E. Fermi", Roma, Italy
[g] Dipartimento di Scienze di Base e Applicate per Ingegneria, Sapienza Università di Roma, Roma, Italy
[h] Center for Life Nano Science@Sapienza, Istituto Italiano di Tecnologia, Roma, Italy
[i] INFN Sezione di Milano, Milano, Italy

ARTICLE INFO

Article history:
Received 20 November 2013
Received in revised form
22 January 2014
Accepted 22 January 2014
Available online 2 February 2014

Keywords:
Gamma detector calibration
Hadrontherapy
Dosimetry

ABSTRACT

Monitoring the dose delivered during proton and carbon ion therapy is still a matter of research. Among the possible solutions, several exploit the measurement of the single photon emission from nuclear decays induced by the irradiation. To fully characterize such emission the detectors need development, since the energy spectrum spans the range above the MeV that is not traditionally used in medical applications. On the other hand, a deeper understanding of the reactions involving gamma production is needed in order to improve the physic models of Monte Carlo codes, relevant for an accurate prediction of the prompt-gamma energy spectrum. This paper describes a calibration technique tailored for the range of energy of interest and reanalyzes the data of the interaction of a 80 MeV/u fully stripped carbon ion beam with a Poly-methyl methacrylate target. By adopting the FLUKA simulation with the appropriate calibration and resolution a significant improvement in the agreement between data and simulation is reported.

1. Introduction

In the last decade, the use of proton and carbon beams has become more and more widespread as an effective therapy for the treatment of solid cancer (hadrontherapy). Due to their very favorable profile of the released dose in tissue, the hadron beams can be very effective in destroying the tumor and sparing the adjacent healthy tissue in comparison to the standard X-ray based treatment [1]. On the other hand, the space selectivity of the hadrontherapy asks for a new approach to the delivered dose monitoring. Indeed, a precise monitoring of the dose is essential for a good quality control of the treatment. Furthermore, the dose monitoring would be particularly useful if provided during the treatment (in-beam monitoring) in order to provide a fast quality check of a treatment.

Several methods have been developed to determine the Bragg Peak position online by exploiting the secondary particle production induced by the hadron beam [2–9]. In this paper we concentrate on the "prompt-photon" method [10–13]: since the irradiation of tissues with hadron beams produces photons within fractions of nanoseconds (prompt photons) by nuclear disexcitations, their rate and production can be related to the released dose profile.

A key element in such studies is the measurement of the energy spectrum of the prompt photons. Ref. [13] presents such a measurement performed by irradiating a Poly-methyl methacrylate (PMMA) target with 80 MeV/u fully stripped carbon ions at the Laboratori Nazionali del Sud (LNS) of the Istituto Nazionale di Fisica Nucleare (INFN) in Catania [13]. For the prompt γs it uses a detector composed of four $1.5 \times 1.5 \times 12\ \mathrm{cm}^3$ crystals of

* Corresponding author at. Dip. Fisica, P.le A. Moro 2, 00185 Rome, Italy. Tel.: +39 06 49914798.
E-mail address: riccardo.faccini@roma1.infn.it (R. Faccini).

http://dx.doi.org/10.1016/j.nima.2014.01.047
0168-9002/

cerium-doped lutetium-yttrium ortho-silicate (LYSO) coupled to an EMI 9814B PMT, read by a 12-bit QDC (CAEN 792N). Such detector was calibrated with the standard ^{22}Na and ^{60}Co sources, emitting 511 keV and 1.17 plus 1.33 MeV photons respectively.

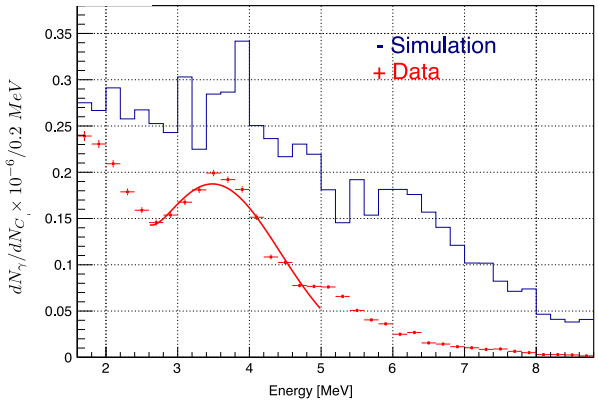

Fig. 1. Energy spectrum of the prompt photons produced by irradiating a PMMA target with 80 MeV/u fully stripped carbon ions as measured in Ref. [13]. The simulation was performed with the GEANT program [14]. The details of the detector response are in Ref. [13].

The measured energy spectrum, including the detector effects discussed in the following, shows that the photons of interest are in the 2–10 MeV range (Fig. 1), and that therefore the calibration was extrapolated to energies higher than those that the sources could provide. Non-linearities in the light yield or in the PMT or in the readout chain could therefore spoil the measurement.

Furthermore, Fig. 1 shows that the Monte Carlo (MC) program used (GEANT [14]) does not properly reproduce the main features of the data. Finally, the only visible structure around 4.4 MeV, due to disexcitation lines of ^{12}C*, ^{11}C*, and ^{11}B* and the corresponding escape lines, is offset in energy with respect to the expected position.

To address these issues left open by the original paper [13], this paper shows an alternative calibration method based on the detection of monochromatic photons of energies up to 9 MeV and the comparison between the measured spectra and rates with an alternative simulation based on the FLUKA program [15].

2. The extended-range calibration

In order to extend the calibration above 1 MeV an indirect production mechanism needs to be implemented since the isotopes

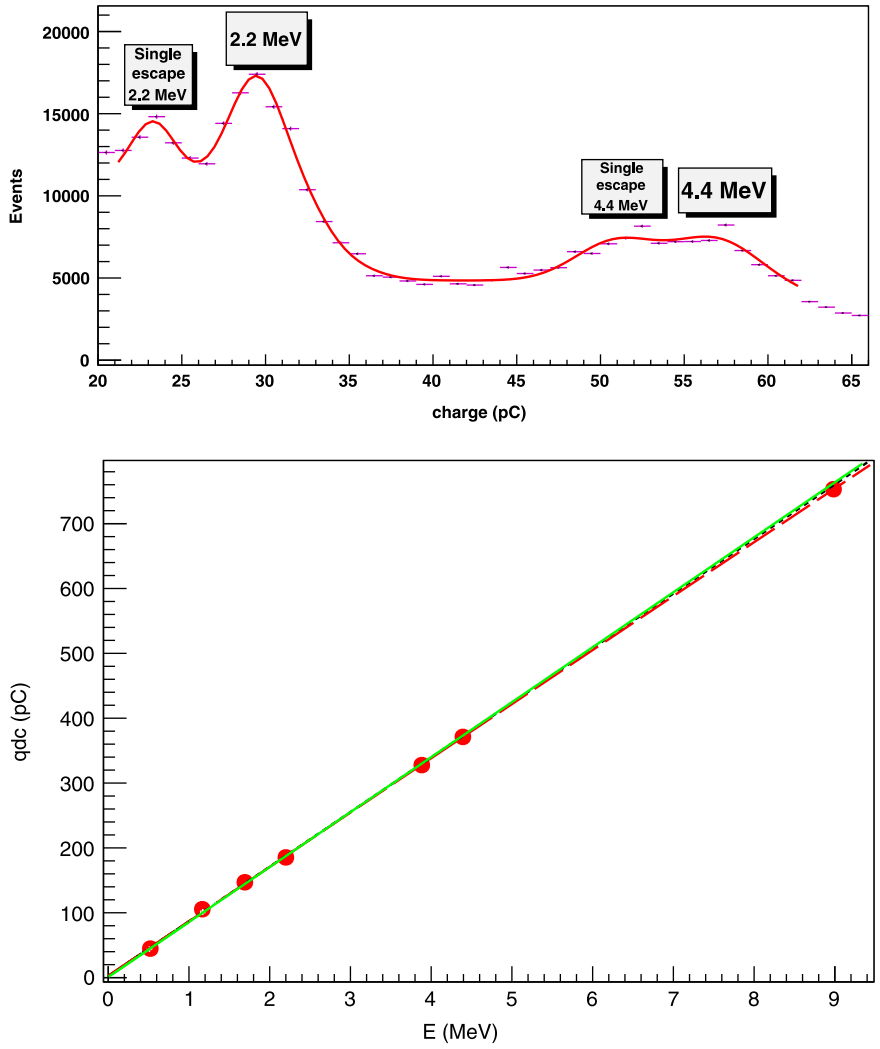

Fig. 2. Top: Example of energy spectrum as obtained with an AmBe source moderated with paraffin with the detector used in Ref. [13]. Bottom: The new calibration curve assuming a linear behavior (dashed red line) compared with the one published in Ref. [13] (full green line). (For interpretation of the references to color in this figure caption, the reader is referred to the web version of this article.)

with high energy γ lines have a very low lifetime. We have therefore exploited the possibility to have neutron induced lines by using an AmBe source that produces approximately 2.5×10^6 n/s. The source was hosted inside a 5 cm thick container made of paraffin ($C_{31}H_{62}$):

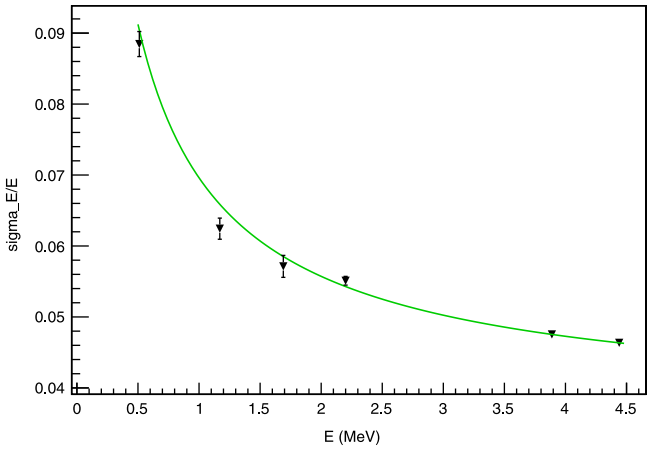

Fig. 3. Dependence of the relative fitted resolution on the energy.

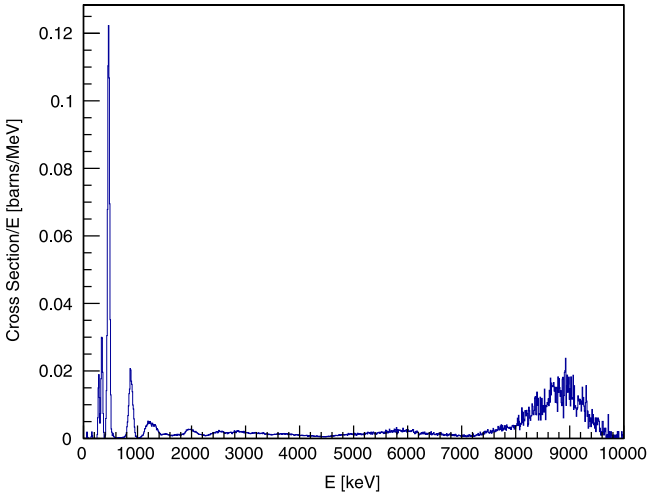

Fig. 4. Expected prompt photon spectrum from neutron irradiation of the natural admixture of Ni obtained by convoluting the nuclear activation lines as tabulated in Ref. [16] and convolving them with the expected resolution.

this allowed both to moderate the neutron flux, that would otherwise blind the detectors, and to produce γ lines. The interaction of the neutrons with the hydrogen produces the 2.22 MeV line from deuteron formation (H(n,γ)d), while the interaction with the carbon produces the 4.44 MeV $^{12}C^*$ disexcitation line.

The measured spectrum is shown in Fig. 2. The 2.22 and 4.44 MeV lines are clearly visible together with the lines that occur when a 511 keV photon produced by the annihilation of a positron escapes the detector (single escape). Each possible signal line has been parametrized in the fit as a Gaussian, while the background is a superposition of Fermi-Dirac functions. This allows to assign a measured value of *ADC* counts to each line and to produce the calibration plot shown in Fig. 2 at the bottom.

From the fit to the spectrum also the resolution as a function of the energy can be obtained. This information is needed as input to the simulation that will be described in the next paragraph. The result is shown in Fig. 3, where the dependence is fitted with

$$\frac{\sigma(E)}{E} = \sqrt{p_0^2 + \frac{p_1^2}{E} + \frac{p_2^2}{E^2}}. \quad (1)$$

We have found the electronic term, p_2, to be consistent with zero, the constant term to be $p_0 = (3.70 \pm 0.007)\%$ and the statistical term to be $p_1 = 0.0579 \pm 0.0006\ \mathrm{MeV}^{1/2}$.

In order to have an additional line for calibration, following Ref. [17] we have also inserted a 2 mm thick rod of nickel between the AmBe source and the detector. The prompt gamma neutron activation of Ni in fact generates a set of high energy lines that can be used for calibration. In order to understand what to expect in the detector, from the knowledge of the cross-sections of all the neutron activated prompt photon lines [16], by taking into account the experimental resolution and the natural abundances, we have simulated the expected γ spectrum resulting from the neutron irradiation of nickel (see Fig. 4). There is a dominant structure at high energy which is due to the superposition of several lines. A Gaussian fit to it returns a mean value of 8795 keV with a 5.2% width. Since the width is larger than the input resolution, it is dominated by the presence of several lines close-by. The effect of escapes is not included in this simulation, but it will be accounted for when fitting the data.

Fig. 5 shows the spectra of the recorded charge in two different runs, one when the nickel rod was superimposed (named "nickel" spectrum in the following) and another one taken in the same identical conditions but without the rod (the "no-nickel" spectrum). The "no-nickel" spectrum is fitted with an exponential

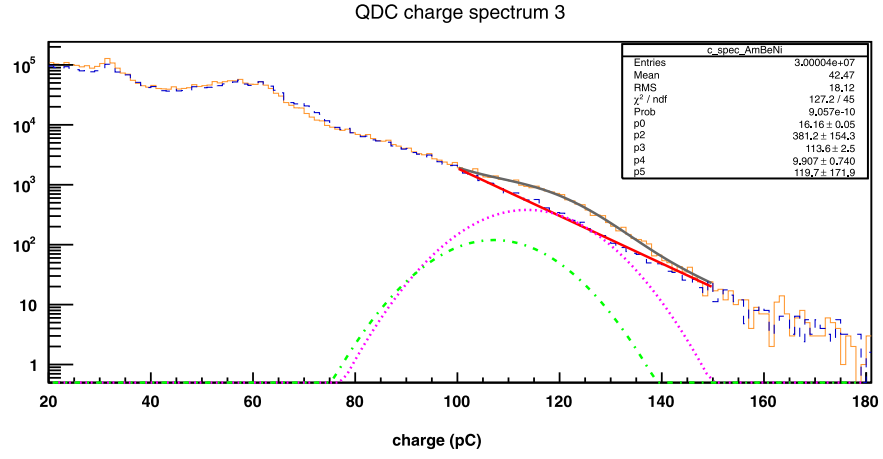

Fig. 5. Observed spectrum with an AmBe source when a nickel rod is interposed (full orange line) and when it is not (dashed blue line). Fits to both spectra as described in the text are superimposed. In the case of the spectrum with nickel, the Gaussian signals from the structure expected at 8.8 MeV (dotted purple line) and its escape (dashed-dotted green line) are shown. (For interpretation of the references to color in this figure caption, the reader is referred to the web version of this article.)

curve representing the background. The "nickel" spectrum is fitted with the sum of an exponential with the same slope as the background one and the sum of two Gaussians representing the Ni structure and its escape respectively. The Gaussian widths are fixed to 5.2% of the mean values as discussed above. The relative offset of the two Gaussians is fixed by the assumption that the escape line is 511 keV below.

From the fits in Figs. 2 and 5 and the previously determined responses to the lines from the ^{22}Na and ^{60}Co sources, the calibration plot of Fig. 2 is obtained. A linear dependence of the *QDC* counts on the energy is verified on the whole range. The same figure also compares this calibration with the one corresponding to Ref. [13] and no significant change is observed.

3. Description of the simulation

Measurements are compared with the 2013.1.0 version of the Monte Carlo code FLUKA [15] simulating the experimental setup described in detail in Ref. [13]. The predefined default 'PRECISIO' is used for the simulation: it enables transport options to enable electromagnetic showers, Rayleigh scattering and inelastic form factor corrections for Compton scatterings with Compton profiles, full analog absorption for low-energy neutrons, and restricted ionization fluctuations. A detailed treatment of the photoelectric edge and fluorescence photons is also activated. Thermal neutrons are transported down to 10^{-5} eV while the other particles are transported down to 100 keV. Delta-ray production threshold is set to 100 keV. Tabulation ratio for hadron and muon dp/dx is set to 1.04; fractional kinetic energy loss per step is set to 0.05.

The beam is simulated as a cylindrical mono-directional source with a 7.5 mm lateral radius, located 25 cm away from the target's nearest face. The geometry has been simplified to reproduce the basic elements, target and *LYSO* detector, which have been described in detail. In order to reduce the contribution of neutrons to the final spectra, the time of flight of each particle between its generation and the arrival to the detector is required to be smaller than 5 ns.

We simulate 6×10^8 impinging carbon ions. To increase the statistics of the results, the detector, made of four LYSO crystals, is virtually replicated in a ring centered in the target and with axis parallel to the beam, with no possible cross detection. The replication is taken into account when normalizing to data statistics. Counts in the scintillator are recorded with a DETECT card, which scores energy deposition on an event by event basis, using a 0.2 MeV binning, to match the experimental data. The scored counts are then folded with the intrinsic resolution of the *LYSO* crystal as determined in Section 2.

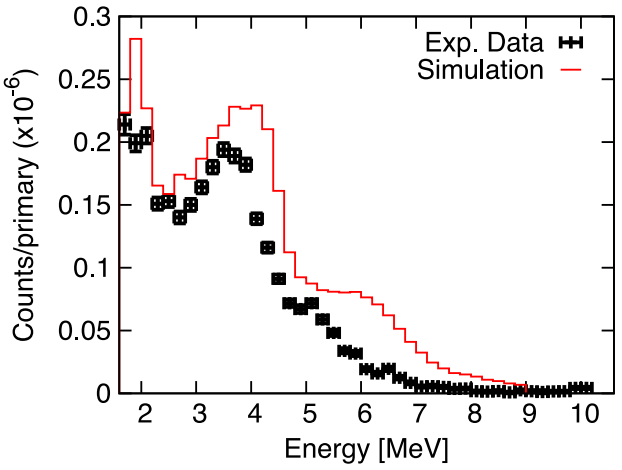

Fig. 6. Comparison between the calibrated spectrum in data (squares) and the FLUKA simulation (histogram).

4. Data-MC comparison

Fig. 6 shows the comparison between the prompt photon energy spectrum after calibration and the FLUKA simulation. As it is clear from Fig. 2, the new calibration procedure has confirmed the original calibration and therefore the data spectrum is fully consistent with the published one (Fig. 1).

As far as the simulation is concerned, in our previous publication the GEANT program could not reproduce well neither the normalization (a 130% excess in simulation) nor the spectrum, in particular in the relative content of the 4.4 MeV line with respect to the rest of the spectrum. The FLUKA simulation reduces the excess in normalization to $\sim$40%, and matches the data well as far as the fraction of 4.4 MeV photons is concerned.

To better quantify this agreement, we studied the composition of the structure around 4.4 MeV due to the ^{12}C*, ^{11}C* and ^{11}B* lines, mixed as a consequence of the resolution of the detector (left Fig. 7). Although the ^{12}C* line constitutes around the 50% of the total height of the peak, the two remaining nuclei contribute significantly. Furthermore, γs can originate both from the PMMA nuclei disexciting almost at rest due to peripheral collisions with the beam ions ("target"), or from projectile fragments, meaning the disexcitations of the excited beam ions and the subsequent fragments. The latter have a high kinetic energy, which causes Doppler broadening of the lines (right Fig. 7).

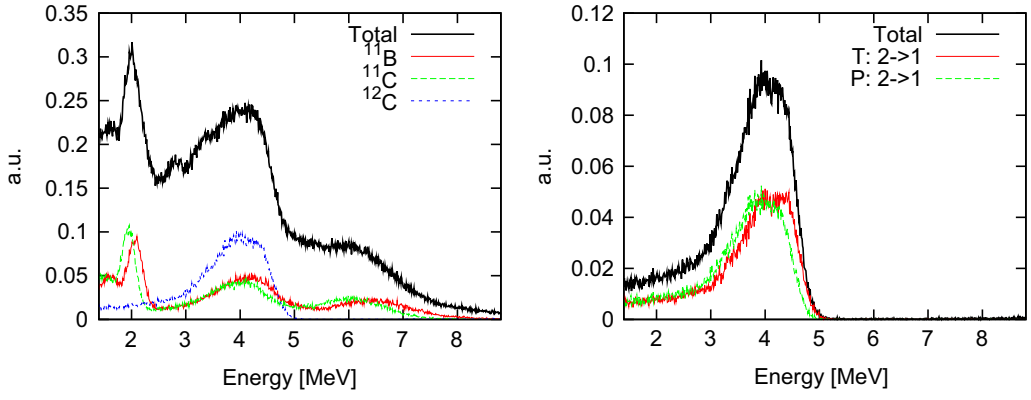

Fig. 7. MC Study with FLUKA. Left: Breakdown of the gamma spectrum among different excited nuclei. Right: Comparison of the target and projectile contributions in the case of ^{12}C* disexcitations.

As far as there comparison with data is concerned we found that $^{12}C^*$ nuclei releasing energy in the [3,5] MeV window account for 14.5% of the prompt photons, number that needs to be compared with the $(13.9 \pm 0.6)\%$ estimated in data [13].

Finally, even using the FLUKA simulation there persists a 10% offset in the energy scale. Given the accuracy of the off-line calibration, the most likely cause is saturation due to a high detection rate. Such effect is not relevant for the dosimetric application that is the goal of this study, but needs to be accounted for when tuning the simulation to the data.

5. Conclusions

We have applied a novel calibration approach exploiting γ lines induced by neutron irradiation of paraffin and nickel: the former provides monochromatic photons of 2.2 and 4.4 MeV, the latter of 9 MeV. This procedure allows to calibrate up to 9 MeV and avoids the need to extrapolate the calibration in the range of interest. With the detectors used in our experiment, 12 cm long LYSO crystals, full linearity of the system was proven. Nonetheless it is important to use this calibration procedure to ascertain possible nonlinearities in the detector.

As far as the simulation is concerned, we showed that the FLUKA simulation reproduces the rate of production of prompt γs and their fraction originating from $^{12}C^*$, $^{11}C^*$, and $^{11}B^*$ decays better than GEANT.

Acknowledgments

The authors would like to thank Dr. M. Pillon and Dr. M. Angelone (ENEA-Frascati, Italy) for allowing us to use the ENEA AmBe source.

References

[1] U. Amaldi, G. Kraft, Reports on Progress in Physics 68 (8) (2005) 1861.
[2] J. Pawelke, et al., IEEE Transactions on Nuclear Science NS-44 (1997) 1492.
[3] K. Parodi, et al., Physics in Medicine and Biology 47 (2002) 21.
[4] W. Enghardt, et al., Nuclear Instruments and Methods in Physics Research Section A 525 (2004) 284.
[5] F. Fiedler, et al., Acta Oncologica 47 (2008) 1077.
[6] S. Vecchio, et al., IEEE Transactions on Nuclear Science NS-56 (2009) 1.
[7] F. Attanasi, Physics in Medicine and Biology 54 (2009) N29.
[8] C. Agodi, et al., Nuclear Instruments and Methods in Physics Research Section B 283 (2012) 18.
[9] C. Agodi, et al., Physics in Medicine and Biology 57 (2012) 5667.
[10] C.H. Min, et al., Applied Physics Letters 89 (2006) 183517.
[11] E. Testa, et al., Nuclear Instruments and Methods in Physics Research Section B 267 (2009) 993.
[12] M. Testa, et al., Radiation and Environmental Biophysics 49 (3) (2010) 337.
[13] C. Agodi, et al., Journal of Instrumentation 7 (2012) P03001.
[14] S. Agostinelli, et al., Spectrometers, Detectors and Associated Equipment: Accelerators 506 (3) (2003) 250;
J. Allison, et al., IEEE Transactions on Nuclear Science NS-53 (February) (2006) 270.
[15] G. Battistoni, et al., The FLUKA code: description and benchmarking, in: Proceedings of the Hadronic Shower Simulation Workshop2006, (2007), aIP Conference Proceedings, vol. 896, 2007, 31.;
A. Ferrari, P.R. Sala, A. Fasso', J. Ranft, FLUKA: A Multi Particle Transport Code, Technical Report CERN-2005-10, INFN/TC05/11, SLAC-R-773, 2005.
[16] International Atomic Energy Agency, Prompt Gamma Neutron Activation Analysis Database, ⟨http://www-nds.iaea.org/pgaa/pgaa7/index.html⟩.
[17] J.G. Rogers, M.S. Andreaco, C. Moisan, I.M. Thorson, Detectors and Associated Equipment 413 (2) (1998) 249;
Se also Sec. 7.1.5 of J. Adam et al.[MEG Collaboration], The MEG detector for $\mu \to e\gamma$ decay search, European Physics Journal C73 (2013) 2365.